

# Transport coefficients of dense nucleon matter at low temperature

---

Jianing Li  and Weiyao Ke 

*Key Laboratory of Quark and Lepton Physics (MOE) & Institute of Particle Physics, Central China Normal University  
Wuhan 430079, China*

*E-mail:* [jianingli@ccnu.edu.cn](mailto:jianingli@ccnu.edu.cn), [weiyaoke@ccnu.edu.cn](mailto:weiyaoke@ccnu.edu.cn)

**ABSTRACT:** Transport properties of cold and dense nucleon matter are important for both nuclear and astrophysics but are relatively less studied than those at finite temperatures. In this paper, we present a primary study of bulk and shear viscosities in the limit  $T/\mu_B \ll 1$ , where  $T$  and  $\mu_B$  are the temperature and the baryon chemical potential. The analysis is performed for a generic system where nucleons are dressed by the condensation of both scalar and vector interactions. Under the relaxation time approximation of the Boltzmann equation, we compute the viscosities of the system to leading power in  $T/\mu_B$  expansion and establish a relation between the thermodynamic potential and transport coefficients, including bulk viscosity ( $\zeta$ ) and shear viscosity ( $\eta$ ). It is found that hydrodynamic stability ( $\zeta > 0$ ) imposes additional constraints on the thermodynamic potential.

As an example, these relations are applied to the Walecka model. The fluid properties of the cold and dense nucleon matter are characterized by the dimensionless combination of viscosities times the quasi-Fermi momentum over the enthalpy. Furthermore, we discuss the implication of the stability condition on the range of applicability of the model.

---

## Contents

<b>1</b>	<b>Introduction</b>	<b>1</b>
<b>2</b>	<b>Transport coefficients of cold and dense fermions</b>	<b>3</b>
2.1	Relaxation time approximation with $T/\mu \ll 1$	3
2.2	Thermodynamics of quasi-particle system within mean field	7
2.3	Extraction of the relaxation time	9
<b>3</b>	<b>Dense nucleon matter at low temperature</b>	<b>10</b>
3.1	Static properties	10
3.2	Transport coefficients	13
<b>4</b>	<b>Conclusion and outlook</b>	<b>16</b>
<b>5</b>	<b>Acknowledgment</b>	<b>17</b>
<b>A</b>	<b>Collision term</b>	<b>17</b>
<b>B</b>	<b>Calculation of the squared scattering amplitude</b>	<b>20</b>

---

## 1 Introduction

In the study of extensive matter governed by quantum chromodynamics (QCD), heavy-ion collisions have attracted considerable attention. The creation of quark-gluon plasma (QGP) and its subsequent evolution become the focal point of the phenomenological study [1–4]. This is because colliding nuclei at relativistic energy produces not only a system at high temperature consisting of quarks and gluons but also a system out of equilibrium, which enables the study of the dynamical response of the QCD matter. At long wavelengths, hydrodynamic theories are an ideal framework for studying its response and provide an elegant explanation for the observed collectivity in relativistic collisions of heavy nuclei [2, 5–9]. The hydrodynamic response is governed by the QCD equation of state and the transport coefficients such as shear and bulk viscosities. These coefficients strongly influence the development of anisotropic flows, identified particle spectra, and many more key observables in experiments at the Relativistic Heavy Ion Collider (RHIC) [10–12] and the Large Hadron Collider (LHC) [13–15].

Understanding the transport properties of nuclear matter is of paramount importance in astrophysics as well. These properties play a crucial role in the dynamics and evolution of compact stellar objects such as neutron stars. The shear and bulk viscosities of dense nuclear matter influence the thermal conductivity, neutrino emission rates, and damping of oscillation modes within neutron stars [16, 17]. These factors are essential for modeling

dissipative phenomena such as neutron star cooling [18–20], magnetic field evolution [21, 22], and the emission of gravitational waves [23, 24]. The discovery of gravitational waves from neutron star mergers by LIGO and Virgo collaborations [25] has intensified the need for precise knowledge of the transport properties of dense matter. Gravitational wave signals provide insights into the equation of state of neutron stars, which depends sensitively on the microscopic interactions and transport coefficients of the nuclear matter composing them [26, 27]. Accurate modeling of these events requires a deep understanding of how shear and bulk viscosities affect the merger dynamics, post-merger oscillations, and the resulting electromagnetic counterparts [28, 29].

Given the importance of accurately describing the transport properties of nuclear matter, numerous studies have made significant contributions to this area [30–36]. One of the most notable predictions is the existence of a lower bound for the ratio of shear viscosity to entropy density in certain type of strongly-coupled field theories, given by  $\eta/s = 1/(4\pi)$  in natural units at infinitely strong coupling, known as the Kovtun–Son–Starinets bound [37]. The proximity of the QGP to this bound has profound implications for our understanding of strongly coupled quantum systems and provides a benchmark for theoretical models [2]. With recent advancements in experimental techniques, understanding the properties of nuclear matter in high-density regions has become increasingly important [38]. Upcoming facilities like the Facility for Antiproton and Ion Research (FAIR), the Nuclotron-based Ion Collider fAcility (NICA), and the High Intensity Heavy-ion Accelerator Facility (HIAF) aim to explore the QCD phase diagram at high baryon densities ( $\mu_B$ ) and low temperatures [39–41]. In these regimes, the created matter resembles the cold and dense nucleon matter found in neutron stars. The temperature of a newly-born neutron star is estimated to be 1–10 MeV [18–20], while those in neutron star merger events are estimated to reach several 10–50 MeV [42, 43]. Both are much lower than the baryon chemical potential of dense neutron matter. Understanding the transport properties in this context is vital for interpreting experimental results and testing theoretical models of dense nuclear matter [44–47]. Meanwhile, next-generation collider experiments, such as those planned at the future Electron-Ion Collider (EIC) and the Electron-Ion Collider in China (EicC) [48, 49], will enable high-precision measurements of the internal dynamics of nucleons and nuclei [50, 51]. These facilities also offer insight into the role of viscosity and other transport properties in the behavior of strongly interacting matter [52–54]. However, there is currently a lack of studies on the transport properties of dense and cold nuclear matter, especially near zero temperature [55]. To fill this gap, we aim to provide a primary prediction for the transport coefficients of dense nucleon matter at temperatures close to zero.

In this work, we investigate the bulk and shear viscosities at low temperatures within the framework of Fermi Liquid Theory. The temperature is assumed to be small enough to define a Fermi surface, yet not too small when the pairing between nucleons becomes important. In Sec. 2, we derive expressions for the transport coefficients of a Fermi liquid, employing the relaxation time approximation (RTA). Due to the non-perturbative nature of QCD at low temperatures and high densities—where lattice QCD calculations are hindered by the infamous sign problem [56]—phenomenological models and effective theories become essential tools for exploring this domain. In light of this, we utilize the Walecka model to

describe the static properties of nucleonic matter [57–60] in Sec. 3. The relaxation time is estimated by calculating tree-level scattering processes in the framework of the Walecka model. Finally, in Sec. 4, we present our conclusions and discuss future outlooks.

## 2 Transport coefficients of cold and dense fermions

### 2.1 Relaxation time approximation with $T/\mu \ll 1$

The relativistic Boltzmann equation for a single-component system in the presence of a collision term  $\mathcal{C}[f]$  is written as [61]

$$\left( \frac{\partial}{\partial t} + \frac{\mathbf{p}}{E_{\mathbf{p}}} \cdot \nabla_{\mathbf{x}} - \nabla_{\mathbf{x}} E_{\mathbf{p}} \cdot \nabla_{\mathbf{p}} \right) f = \mathcal{C}[f], \quad (2.1)$$

where we consider  $f \equiv f(x^\mu, p^\mu)$  is the fermionic distribution function, with  $x^\mu = (t, \mathbf{x})$  and  $p^\mu = (E_{\mathbf{p}}, \mathbf{p})$  representing the spacetime coordinates and four-momentum of the fermions, respectively. The zeroth component of  $p^\mu$  is the energy  $E_{\mathbf{p}} = \sqrt{\mathbf{p}^2 + m^2}$ , where  $m$  is the mass. With the metric defined as  $g^{\mu\nu} = \text{diag}(1, -1, -1, -1)$ , the symmetric energy-momentum tensor is expressed as

$$T^{\mu\nu} = -pg^{\mu\nu} + (p + \varepsilon) u^\mu u^\nu + \delta T^{\mu\nu}, \quad (2.2)$$

where  $p$  is the pressure,  $\varepsilon$  is the energy density, and  $u^\mu$  is the four-velocity of the fluid cell. Furthermore, the dissipative term  $\delta T^{\mu\nu}$  satisfies the Landau–Lifshitz condition  $u_\mu \delta T^{\mu\nu} = 0$ .

At the first order of the gradient expansion, we have

$$\Pi^{\mu\nu} = \eta \left( D^\mu u^\nu + D^\nu u^\mu + \frac{2}{3} \Delta^{\mu\nu} \vartheta \right) - \zeta \Delta^{\mu\nu} \vartheta, \quad (2.3)$$

where we define  $\vartheta = \partial \cdot u$ . Here,  $\Delta^{\mu\nu} = u^\mu u^\nu - g^{\mu\nu}$  is the projection tensor, and  $D_\mu = \partial_\mu - u_\mu u \cdot \partial$  is the derivative normal to  $u^\mu$ . It is useful to express these projections in the local rest frame, i.e.,  $u^\mu = (1, 0, 0, 0)$ ,

$$\Delta^{0\nu} = 0, \quad \Delta^{ij} = \delta^{ij}, \quad D_0 = 0, \quad D_i = \partial_i. \quad (2.4)$$

The prefactors  $\eta$  and  $\zeta$  are the *shear viscosity* and *bulk viscosity*, respectively.

In a system of well-defined quasi-particles, the energy-momentum tensor (neglecting residue interactions) is expressed as

$$T^{\mu\nu} = \sum_i \int \frac{d^3\mathbf{p}}{(2\pi)^3} \frac{p^\mu p^\nu}{E_{\mathbf{p}}} f_i. \quad (2.5)$$

where  $i$  sums over all quantum numbers with degeneracies. For a system of free relativistic fermion, the equilibrium distribution is typically given as<sup>1</sup>

$$\begin{aligned} f_0(x, p) &= \frac{1}{\exp[\beta(u \cdot p - \mu)] + 1} \\ &= \Theta(\mu - u \cdot p) + \mathcal{O}(T^2/\mu^2), \end{aligned} \quad (2.6)$$

<sup>1</sup>Due to the general formula presented in this section, the chemical potential is represented by  $\mu$  instead of specifying a particular baryon type  $\mu_B$  in Sec. 3.

where  $\beta = 1/T$  is the inverse of temperature  $T$ , and  $\mu$  is the chemical potential of a conserved charge<sup>2</sup>. In the second line, we have power expanded the distribution function in  $T/\mu$ . Assuming that  $f$  deviates slightly from equilibrium, we can decompose the particle distribution into  $f = f_0 + \delta f$ , where  $\delta f$  is the non-equilibrium correction term.

Even though Eq. (2.6) describes a non-interacting many-particle system, which differs from a real-world system, it provides qualitative explanations for salient features of the latter. In 1956, Lev Landau introduced the *Landau Fermi Liquid Theory* (LFLT) to explain the low-temperature behavior of interacting fermion systems, such as electrons in metals [62]. The theory centers around the concept of quasi-particles, fermion-like excitations, that retain essential properties of free fermions but are modified by interactions [63, 64]. The system's behavior can still be described using Fermi–Dirac statistics with an effective mass  $m^*$  and an effective Fermi surface  $\mu^*$  modified by interaction, as illustrated in Figure 1. This theory has been instrumental in explaining various physical properties of metals

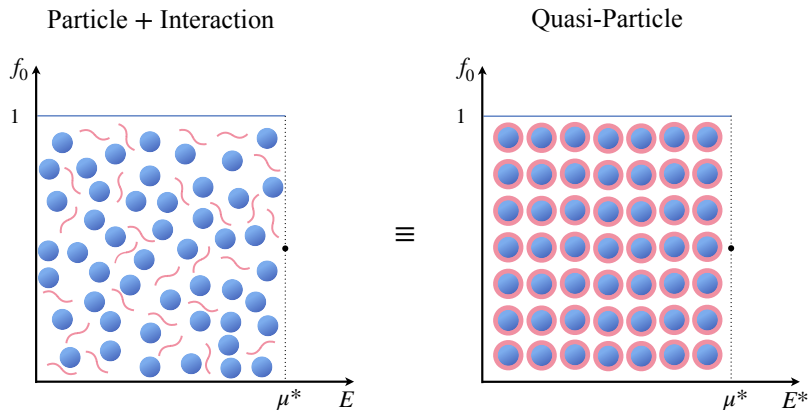


**Figure 1.** A schematic representation of Fermi liquid at zero temperature. Left: bare particles and interactions. Right: quasi-particles with effective mass  $m^*$  and effective chemical potential  $\mu^*$ .

and liquid helium-3, including specific heat and magnetic susceptibility, making it a cornerstone of condensed matter physics [65]. There are also numerous LFLT applications to study nuclear matter at the finite density from low-energy effective models of the strong interaction [66–77].

Usually, in the mean-field approximation (MFA) of such an effective model for relativistic fermions, modifications in  $m^*$  and  $\mu^*$  are introduced due to spontaneous symmetry breaking in the scalar and vector channel interactions, respectively. Without loss of generality, we assume

$$m^* = m + \mathcal{f}(\bar{\sigma}) , \quad \mu^* = \mu + \mathcal{g}(\bar{\omega}_0) . \quad (2.7)$$

<sup>2</sup>For anti-particles,  $\mu$  is replaced by  $-\mu$  in Eq. (2.5). However, for cold systems with  $\mu/T \gg 1$ , we will neglect the anti-particle contributions hereafter.

Here,  $\bar{\sigma}$  and  $\bar{\omega}_0$  are the scalar and vector condensates that account for spontaneous symmetry breaking. For simplicity, the vector condensate has been rotated to the zeroth component. The functions  $\mathcal{L}(\cdot)$  and  $\mathcal{G}(\cdot)$  are dressing functions for the scalar and vector channels.

At zero temperature, the local equilibrium distribution function is given by  $f_0 = \Theta(\mu^* - u \cdot p)$ , where  $E_{\mathbf{p}}^* = \sqrt{m^{*2} + \mathbf{p}^2}$ . The effective quantities  $\mu^*$  and  $m^*$  both depend on the chemical potential  $\mu$ . In a system out of the global equilibrium, we consider a chemical potential  $\mu(x^\mu)$  that slowly varies in spacetime, thus both  $\mu^*[\mu(x^\mu)]$  and  $m^*[\mu(x^\mu)]$  are functions of the spacetime coordinates as well. Out-of-local-equilibrium effects can be thought of as the distortion of the shape of the fermi surface at each point in spacetime. At finite but low temperatures, we can power expand the calculations in the small parameter  $T/\mu^*$  and the arguments above still hold for at the zeroth order.

For long-wavelength excitations at zero temperature, Ref. [78] shows that (for the non-relativistic system) the deviation from the local equilibrium distribution  $f_0$  could be parameterized as deformations of the Fermi surfaces,

$$f_0 + \delta f(T = 0) = \Theta(p_F - |\mathbf{p}|) + \delta(p_F - |\mathbf{p}|) \mathbf{n}_\theta \cdot \nabla_{\mathbf{x}} \Phi(\mathbf{x}, \mathbf{n}_\theta) + \dots, \quad (2.8)$$

where  $\mathbf{n}_\theta = \mathbf{p}/|\mathbf{p}|$  is a unit vector, and the structure of the deformation term follows from the canonical symmetry of the transport part in the Boltzmann equation. At vanishing temperature, non-forward scatterings are completely suppressed and the systems have an infinite number of conserved quantities and their corresponding hydrodynamic modes, labeled by  $\theta$ . At finite temperature, off-forward scatterings introduce small but finite breaking of the canonical transformation symmetry to the Boltzmann equation; therefore, one expects 1) a reduction of the number of conserved quantities, 2) the form in Eq. (2.8) will be generalized by terms that were previously not allowed by canonical symmetry, 3) such terms are suppressed by powers of  $T/\mu$ . For this reason, we start from a more general form of deviations around the Fermi surface,

$$f_0 + \delta f(T \neq 0) = \Theta(\mu^* - u \cdot p) + \delta(\mu^* - u \cdot p) \phi + \dots \quad (2.9)$$

with a consideration of the Lorentz covariance.

Returning to the Boltzmann equation in Eq. (2.1), we first power expand the distribution function in  $T/\mu$ , and then write down the equation to the first order of the deviation  $\delta f$

$$-\frac{1}{E_{\mathbf{p}}^*} \left[ p^\mu (p \cdot \partial) u_\mu - \frac{d\mu^*}{d\mu} p \cdot \partial \mu + m^* \frac{dm^*}{d\mu} u \cdot \partial \mu \right] \delta(\mu^* - u \cdot p) = \mathcal{C}[\delta f], \quad (2.10)$$

Adopting the RTA, the collision term can be expressed as  $\mathcal{C}[f] = -\delta f/\tau_{\text{rel}}$ , where the relaxation time  $\tau_{\text{rel}}$  depends on the detail of interaction. Then,  $\phi$  is solved by

$$\phi = \frac{\tau_{\text{rel}}}{E_{\mathbf{p}}^*} \left[ p^\mu (p \cdot \partial) u_\mu - \frac{d\mu^*}{d\mu} p \cdot \partial \mu + m^* \frac{dm^*}{d\mu} u \cdot \partial \mu \right]. \quad (2.11)$$

To eliminate the temporal derivative, we employ the ideal hydrodynamic equation of motion. Using the thermodynamic relation  $\varepsilon = Ts - p + \mu^* n^*$  and  $n^* = \partial p / \partial \mu^*$ , the conservation

laws, i.e.,  $\partial_\mu T^{\mu\nu} = 0$  and  $\partial_\mu (n^* u^\mu) = 0$ , at  $T = 0$  give<sup>3</sup>

$$\mu^* u \cdot \partial u^\nu + \Delta^{\mu\nu} \partial_\mu \mu^* = 0. \quad (2.12)$$

Building upon this, the solution takes the form

$$\partial_\mu \ln \mu^* = u \cdot \partial u_\mu + \xi u_\mu \vartheta. \quad (2.13)$$

By applying the conservation law of the energy-momentum tensor,  $u_\nu \partial_\mu T^{\mu\nu} = 0$ , we obtain

$$\xi = -\frac{n^*}{d\varepsilon/d\mu^*}. \quad (2.14)$$

Using the thermodynamic relation  $n^* = dp/d\mu^*$  and the definition of the square of the sound velocity  $v_s^2 = dp/d\varepsilon$ , we can show that

$$\xi = -\frac{dp/d\mu^*}{d\varepsilon/d\mu^*} = -v_s^2, \quad (2.15)$$

and therefore,

$$\partial_\mu \mu = \mu^* \left( u \cdot \partial u_\mu - v_s^2 u_\mu \vartheta \right) \frac{d\mu}{d\mu^*}. \quad (2.16)$$

From this expression, we can derive

$$\phi = \frac{\tau_{\text{rel}}}{E_{\mathbf{p}}^*} \left[ (p \cdot \partial) (u \cdot p) - \mu^* (u \cdot \partial) (u \cdot p) + v_s^2 \mu^* \left( u \cdot p - m^* \frac{dm^*}{d\mu^*} \right) \vartheta \right]. \quad (2.17)$$

As a result, the non-equilibrium correction  $\delta f$  can be decomposed into

$$\delta f = \phi_1 p^\rho p^\sigma \left( D_\rho u_\sigma + D_\sigma u_\rho + \frac{2}{3} \Delta_{\rho\sigma} \vartheta \right) - \phi_2 \vartheta, \quad (2.18)$$

with coefficients

$$\phi_1 = \frac{\tau_{\text{rel}}}{2E_{\mathbf{p}}^*} \delta(\mu^* - u \cdot p), \quad (2.19a)$$

$$\phi_2 = \frac{\tau_{\text{rel}}}{3E_{\mathbf{p}}^*} \delta(\mu^* - p \cdot u) \left\{ (p \cdot u)^2 \left[ 1 - 3v_s^2 \left( 1 - \frac{m^*}{\mu^*} \frac{dm^*}{d\mu^*} \right) \right] - m^{*2} \right\}. \quad (2.19b)$$

Note that in the non-relativistic limit, the form of the solution can indeed be cast back to the ansatz given in Eq. (2.8). Considering that the viscous part of the energy-momentum tensor in the local rest frame of the fluid is given by

$$\Pi^{\mu\nu} = \int \frac{d^3\mathbf{p}}{(2\pi)^3} \frac{p^\mu p^\nu}{E_{\mathbf{p}}^*} \delta f, \quad (2.20)$$

we obtain expressions for the shear viscosity  $\eta$  and bulk viscosity  $\zeta$  as

$$\eta = \frac{2}{15} \int \frac{d^3\mathbf{p}}{(2\pi)^3} \frac{\mathbf{p}^4}{E_{\mathbf{p}}^*} \phi_1, \quad (2.21a)$$

$$\zeta = \frac{1}{3} \int \frac{d^3\mathbf{p}}{(2\pi)^3} \frac{\mathbf{p}^2}{E_{\mathbf{p}}^*} \phi_2. \quad (2.21b)$$

---

<sup>3</sup>Note in the relation  $\partial_\mu (n^* u^\mu) = 0$  we adopt  $\mu^*$  for the Lagrange multiplier.

## 2.2 Thermodynamics of quasi-particle system within mean field

Before proceeding further, we would like to discuss some specific thermodynamic quantities of dense and cold fermions. For free fermions at zero temperature, the pressure  $p_0$ , energy density  $\varepsilon_0$ , and particle number density  $n_0$  are given by [79]

$$p_0(\mu, m) = \frac{2s+1}{48\pi^2} \left[ |\mu| (2\mu^2 - 5m^2) \sqrt{\mu^2 - m^2} + 3m^4 \cosh^{-1} \left( \frac{|\mu|}{m} \right) \right] \Theta(|\mu| - m), \quad (2.22a)$$

$$\varepsilon_0(\mu, m) = \frac{2s+1}{16\pi^2} \left[ |\mu| (2\mu^2 - m^2) \sqrt{\mu^2 - m^2} - m^4 \cosh^{-1} \left( \frac{|\mu|}{m} \right) \right] \Theta(|\mu| - m), \quad (2.22b)$$

$$n_0(\mu, m) = (2s+1) \frac{(\mu^2 - m^2)^{\frac{3}{2}}}{6\pi^2} \Theta(|\mu| - m), \quad (2.22c)$$

with  $s$  corresponding to the intrinsic spin of the fermion and the inverse hyperbolic cosine function expressed as  $\cosh^{-1}(z) = \ln(z + \sqrt{z^2 - 1})$ . Based on these expressions, the squared speed of sound  $v_s^2$  as a function of  $m$  and  $\mu$  is calculated as<sup>4</sup>

$$v_s^2 = \frac{1}{3} \left( 1 - \frac{m^2}{\mu^2} \right) \Theta(|\mu| - m). \quad (2.23)$$

As  $m$  approaches zero,  $v_s$  converges to the characteristic speed of sound in a massless Fermi gas, which is  $1/\sqrt{3}$ . With this, we have

$$\phi_2 = \frac{\tau_{\text{rel}}}{3E_{\mathbf{p}}^*} \delta(\mu^* - p \cdot u) \left( \mu^{*2} - m^{*2} \right) \frac{m^*}{\mu^*} \frac{dm^*}{d\mu^*}. \quad (2.24)$$

From this, we can notice that the sign of  $\zeta$  is determined by  $dm^*/d\mu^*$ . In the MFA, the effective potential  $\bar{\mathcal{V}}_{\text{eff}}$  can generally be expressed as

$$\bar{\mathcal{V}}_{\text{eff}}(\mu; \bar{\sigma}, \bar{\omega}_0) = -p(\mu; \bar{\sigma}, \bar{\omega}_0) = - \sum_i p_0[m_i^*(\bar{\sigma}), \mu_i^*(\bar{\omega})] + \mathcal{U}(\bar{\sigma}, \bar{\omega}_0), \quad (2.25)$$

where the subscript  $i$  sums over all particle species. The residual interaction contributions in the MFA are encapsulated in the potential  $\mathcal{U}$ . The condensates  $\bar{\sigma}$  and  $\bar{\omega}_0$  are determined self-consistently by the gap equations obtained from extremum conditions

$$q_1[m^*(\bar{\sigma}), \bar{\sigma}, \mu^*] = \frac{\partial \bar{\mathcal{V}}_{\text{eff}}}{\partial \bar{\sigma}} \equiv 0, \quad (2.26a)$$

$$q_2[m^*, \mu^*(\bar{\omega}_0), \bar{\omega}_0] = \frac{\partial \bar{\mathcal{V}}_{\text{eff}}}{\partial \bar{\omega}_0} \equiv 0. \quad (2.26b)$$

Furthermore, to ensure the stability of the thermodynamic system, the following conditions must be met:

$$\begin{vmatrix} \frac{\partial^2 \bar{\mathcal{V}}_{\text{eff}}}{\partial \bar{\sigma}^2} & \frac{\partial^2 \bar{\mathcal{V}}_{\text{eff}}}{\partial \bar{\sigma} \partial \bar{\omega}_0} \\ \frac{\partial^2 \bar{\mathcal{V}}_{\text{eff}}}{\partial \bar{\omega}_0 \partial \bar{\sigma}} & \frac{\partial^2 \bar{\mathcal{V}}_{\text{eff}}}{\partial \bar{\omega}_0^2} \end{vmatrix} > 0, \quad (2.27a)$$

<sup>4</sup>In Eqs. (2.22, 2.23), the absolute value of the chemical potential is for the general expression.



$$\frac{\partial^2 \bar{\mathcal{V}}_{\text{eff}}}{\partial \bar{\sigma}^2} > 0. \quad (2.27b)$$

To calculate  $dm^*/d\mu^*$ , we use the condition

$$\frac{dq_1}{d\mu} = \frac{dq_2}{d\mu} = 0, \quad (2.28)$$

which leads to

$$\left[ \frac{\partial q_1}{\partial m^*} + \frac{1}{f'(\bar{\sigma})} \frac{\partial q_1}{\partial \bar{\sigma}} \right] \frac{dm^*}{d\mu} + \frac{\partial q_1}{\partial \mu^*} \frac{d\mu^*}{d\mu} = 0, \quad (2.29a)$$

$$\frac{\partial q_2}{\partial m^*} \frac{dm^*}{d\mu} + \left[ \frac{\partial q_2}{\partial \mu^*} + \frac{1}{g'(\bar{\omega}_0)} \frac{\partial q_2}{\partial \bar{\omega}_0} \right] \frac{d\mu^*}{d\mu} = \frac{1}{g'(\bar{\omega}_0)} \frac{\partial q_2}{\partial \bar{\omega}_0}. \quad (2.29b)$$

Solving these equations, we find

$$\frac{dm^*}{d\mu} = - \frac{\frac{\partial q_1}{\partial \mu^*} \cdot \frac{1}{g'(\bar{\omega}_0)} \frac{\partial q_2}{\partial \bar{\omega}_0}}{\left[ \frac{\partial q_1}{\partial m^*} + \frac{1}{f'(\bar{\sigma})} \frac{\partial q_1}{\partial \bar{\sigma}} \right] \left[ \frac{\partial q_2}{\partial \mu^*} + \frac{1}{g'(\bar{\omega}_0)} \frac{\partial q_2}{\partial \bar{\omega}_0} \right] - \frac{\partial q_1}{\partial \mu^*} \frac{\partial q_2}{\partial m^*}}, \quad (2.30a)$$

$$\frac{d\mu^*}{d\mu} = \frac{\left[ \frac{\partial q_1}{\partial m^*} + \frac{1}{f'(\bar{\sigma})} \frac{\partial q_1}{\partial \bar{\sigma}} \right] \frac{1}{g'(\bar{\omega}_0)} \frac{\partial q_2}{\partial \bar{\omega}_0}}{\left[ \frac{\partial q_1}{\partial m^*} + \frac{1}{f'(\bar{\sigma})} \frac{\partial q_1}{\partial \bar{\sigma}} \right] \left[ \frac{\partial q_2}{\partial \mu^*} + \frac{1}{g'(\bar{\omega}_0)} \frac{\partial q_2}{\partial \bar{\omega}_0} \right] - \frac{\partial q_1}{\partial \mu^*} \frac{\partial q_2}{\partial m^*}}. \quad (2.30b)$$

From this, we can solve for

$$\frac{dm^*}{d\mu^*} = \frac{dm^*/d\mu}{d\mu^*/d\mu} = - \frac{f'(\bar{\sigma})}{g'(\bar{\omega}_0)} \frac{\partial^2 \bar{\mathcal{V}}_{\text{eff}}}{\partial \bar{\omega}_0 \partial \bar{\sigma}} \left( \frac{\partial^2 \bar{\mathcal{V}}_{\text{eff}}}{\partial \bar{\sigma}^2} \right)^{-1}. \quad (2.31)$$

With the quasi-Fermi momentum defined as  $p_F^* = \sqrt{\mu^{*2} - m^{*2}}$ , the transport coefficients can be expressed as

$$\eta = \frac{p_F^{*5}}{30\pi^2 \mu^*} \tau_{\text{rel}}(\mu^*), \quad (2.32a)$$

$$\zeta = - \frac{p_F^{*5}}{18\pi^2 \mu^*} \frac{m^* f'(\bar{\sigma})}{\mu^* g'(\bar{\omega}_0)} \frac{\partial^2 \bar{\mathcal{V}}_{\text{eff}}}{\partial \bar{\omega}_0 \partial \bar{\sigma}} \left( \frac{\partial^2 \bar{\mathcal{V}}_{\text{eff}}}{\partial \bar{\sigma}^2} \right)^{-1} \tau_{\text{rel}}(\mu^*). \quad (2.32b)$$

We note that the condition for the positive definiteness of the transport coefficients imposes that

$$\frac{f'(\bar{\sigma})}{g'(\bar{\omega}_0)} \frac{\partial^2 \bar{\mathcal{V}}_{\text{eff}}}{\partial \bar{\omega}_0 \partial \bar{\sigma}} \left( \frac{\partial^2 \bar{\mathcal{V}}_{\text{eff}}}{\partial \bar{\sigma}^2} \right)^{-1} < 0 \quad (2.33)$$

which is an independent constraint from the stability conditions of the thermal-dynamical potential given in Eqs. (2.27). This is a somewhat surprising result. Because the positivity of transport coefficient ensures a positive definite local entropy production rate. Therefore the evolution of the system is dissipative and stable. On the other hand, the stability of the global thermodynamic stability is given by Eqs. (2.27). So we would imagine that the two sets of conditions are related to each other. However, Eq. (2.33) and Eqs. (2.27) are independent sets of conditions. It is possible that this is an artifact of the use of RTA of the collision term. In future works, we will go beyond the RTA collision terms and investigate the positivity condition of the bulk viscosity.

### 2.3 Extraction of the relaxation time

In this section, we extract the relaxation time  $\tau_{\text{rel}}$  used in the RTA collision term from the full collision term that includes  $2 \leftrightarrow 2$  scattering processes of identical fermions. We designate the incoming particles as  $a$  and  $b$ , and the outgoing particles as  $c$  and  $d$ . In the previous formulas,  $E_{\mathbf{p}}^*$  should now be replaced by  $E_a^*$ . For spin-1/2 fermions, the collision term can be expressed as

$$\mathcal{C}[f] = \frac{1}{2} \frac{1}{2E_a^*} \int_{\mathbf{p}_b, \mathbf{p}_c, \mathbf{p}_d} [W(a+b \rightarrow c+d) f_c f_d \bar{f}_a \bar{f}_b - W(c+d \rightarrow a+b) f_a f_b \bar{f}_c \bar{f}_d], \quad (2.34)$$

where  $\bar{f}_i = 1 - f_i$ , and we have abbreviated the integration measure as  $\int_{\mathbf{p}} \equiv \int d^3\mathbf{p} / [2E_{\mathbf{p}} (2\pi)^3]$ , and  $\int_{\mathbf{p}_1, \dots, \mathbf{p}_n} \equiv \int \prod_{i=1}^n d^3\mathbf{p}_i / [2E_{\mathbf{p}_i} (2\pi)^3]$ . The prefactor  $1/2$  accounts for identical incoming particles. The collision kernel is given by

$$W(i+j \rightarrow k+l) = \frac{1}{4} \sum_{\text{spin}} |\mathcal{M}|^2 (2\pi)^4 \delta(p_i + p_j - p_k - p_l), \quad (2.35)$$

with  $\mathcal{M}$  being the scattering amplitude. Considering unpolarized scattering, we sum over the spins in the initial and final states, and the factor  $1/4$  is for averaging over initial spins. From the detailed balance principle, we have  $W(a+b \leftrightarrow c+d) \equiv W(a+b \rightarrow c+d) = W(c+d \rightarrow a+b)$ . To maintain consistency with the left-hand side of the Boltzmann equation, we perform a linear expansion of  $\delta f_a$ . Consequently, the collision term in Eq. (2.34) transforms into

$$\mathcal{C}[f] = -\omega(E_a^*) \delta f_a, \quad (2.36)$$

where the typical relaxation frequency is calculated as<sup>5</sup>

$$\omega(E_a^*) = \frac{1}{2} \frac{1}{2E_a^*} \int_{\mathbf{p}_b, \mathbf{p}_c, \mathbf{p}_d} W(a+b \leftrightarrow c+d) (f_{0c} f_{0d} \bar{f}_{0b} + f_{0b} \bar{f}_{0c} \bar{f}_{0d}). \quad (2.37)$$

From this, we can estimate the relaxation time via  $\tau_{\text{rel}} = 1/\omega$ .

Since all states are occupied under the Fermi surface in a fermionic system at exactly zero temperature, no state beyond this energy can be occupied. The collisions near the Fermi surface are forbidden by the conservation of energy, resulting in a vanishing viscosity. The evolution of the system causes no increase in entropy, which is also compatible with the third law of thermodynamics of  $s(T=0) = 0$ .

At a finite yet negligible temperature ( $T/\mu^* \ll 1$ ), the distribution functions can be expanded in powers of  $T/\mu^*$  to determine  $\omega$ . This approach is analogous to applying the Sommerfeld expansion to an integral involving the Fermi–Dirac distribution [80]. Within this framework, the equilibrium distribution function can be decomposed

$$f_{0i} = \Theta(\mu^* - E_i^*) + \delta f_{0i}, \quad (2.38)$$

---

<sup>5</sup>Henceforth,  $f_{0i}$  will denote the equilibrium distribution function of particle  $i$ .

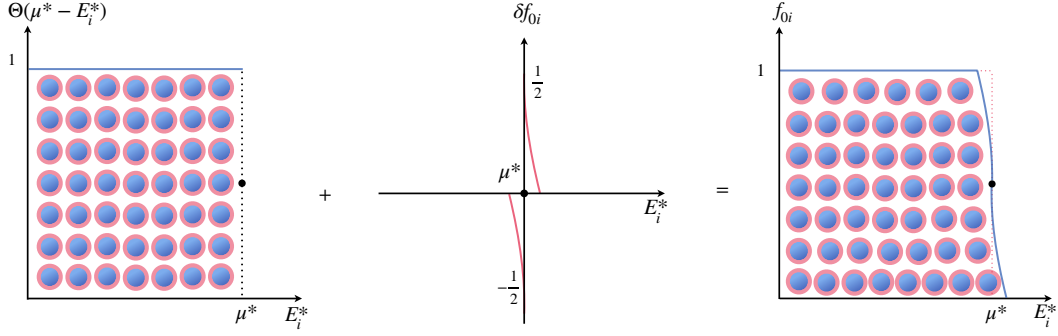


**Figure 2.** A sketch of the Sommerfeld expansion at  $T/\mu^* \ll 1$ .

with

$$\delta f_{0i} = -\frac{(\pi T)^2}{6} \delta'(E_i^* - \mu^*) + \mathcal{O}\left(\frac{T^4}{\mu^{*4}}\right) \quad (2.39)$$

Figure 2 is a schematic plot of such an expansion. In the product of particle distributions in Eq. (2.37), the term consisting solely of the zeroth-order contributions vanishes due to the absence of available states to accommodate outgoing particles. Accordingly, the detailed balance process in the same order also vanishes. Beyond the zeroth order, it can be observed that the term at order  $T^2$  is raised from  $f_{0c}f_{0d}\bar{f}_{0b}$ , as it primarily stems from the occupancy effect predominantly influenced by density. In contrast, the detailed balance term  $f_{0b}\bar{f}_{0c}\bar{f}_{0d}$  contributes only from order  $T^4$ , since the inverse process is governed by thermal excitations. As a result, we retain only the leading-order contribution in the non-vanishing distributions, which is computed as

$$\begin{aligned} f_{0c}f_{0d}\bar{f}_{0b} \approx & -\Theta(\mu^* - E_c^*)\Theta(\mu^* - E_d^*)\delta f_{0b} + \Theta(\mu^* - E_d^*)\Theta(E_b^* - \mu^*)\delta f_{0c} \\ & + \Theta(\mu^* - E_c^*)\Theta(E_b^* - \mu^*)\delta f_{0d}. \end{aligned} \quad (2.40)$$

The collision term is calculated in the rest frame of the fluid cell. More details of the calculation are provided in Appendix A.

### 3 Dense nucleon matter at low temperature

#### 3.1 Static properties

Protons and neutrons serve as the primary fermionic degrees of freedom in this study. The nuclear force is inherently complex, featuring long-range meson-mediated attractions alongside short-range repulsive interactions that are pivotal for achieving the saturation density of nuclear matter. To accurately model these phenomena, we adopt the Walecka model [57], a relativistic mean-field theory renowned for its ability to describe the binding and saturation characteristics of nuclear systems. Through the inclusion of both scalar

and vector meson exchanges, the Walecka model offers a comprehensive framework for investigating the equation of state of nuclear matter under diverse conditions [58–60].

The Lagrangian density of the Walecka model is composed of  $\mathcal{L}_W = \mathcal{L}_f + \mathcal{L}_{\text{int}}$  wherein the fermion (nucleon) part  $\mathcal{L}_f$  and the interaction term  $\mathcal{L}_{\text{int}}$  are respectively given by

$$\mathcal{L}_f = \sum_{N=n,p} \bar{\psi}_N (i\cancel{\partial} - m_N + g_\sigma\sigma - g_\omega\cancel{\omega} + \mu_B\gamma_0) \psi_N, \quad (3.1a)$$

$$\mathcal{L}_{\text{int}} = \frac{1}{2} (\partial_\mu\sigma\partial^\mu\sigma - m_\sigma^2\sigma^2) - U(\sigma) - \frac{1}{4}F^{\mu\nu}F_{\mu\nu} + \frac{1}{2}m_\omega^2\omega^\mu\omega_\mu, \quad (3.1b)$$

where  $F_{\mu\nu} = \partial_\mu\omega_\nu - \partial_\nu\omega_\mu$  and  $\psi_N$  ( $N = n, p$ ) denotes the nucleon fields, with  $n$  representing neutrons and  $p$  for protons. In present frame, isospin symmetry is assumed for simplicity, so that both of mass are  $m_N$ . The scalar  $\sigma$  meson with mass  $m_\sigma$  and the vector  $\omega$  meson with mass  $m_\omega$  are included to account for the long-range attraction and short-range repulsion of the nuclear force, respectively. These interactions are captured by the meson-nucleon coupling terms, with coupling constants  $g_\sigma$  and  $g_\omega$ . Additionally, we introduce a phenomenological potential [81]

$$U(\sigma) = \frac{1}{3}bm_N(g_\sigma\sigma)^3 + \frac{1}{4}c(g_\sigma\sigma)^4 \quad (3.2)$$

to fit the empirically observed properties of nuclear matter. Currently, the conserved charge is the net baryon number  $B$ , so we then specify the chemical potential and particle density as baryonic, i.e.,  $\mu \rightarrow \mu_B$ ,  $\mu^* \rightarrow \mu_B^*$ ,  $n^* \rightarrow n_B^*$  and the mass as that of the nucleon, i.e.,  $m^* \rightarrow m_N^*$ .

The partition function of the model can be expressed in the imaginary-time path integral formalism,

$$\mathcal{Z}_W = \int \prod_{N=n,p} [d\psi_N][d\bar{\psi}_N][d\sigma][d\omega_\mu] e^{\int_0^\beta d\tau \int d^3\mathbf{x} (\mathcal{L}_W + \mu_B \sum_{N=n,p} \psi_N^\dagger \psi_N)}. \quad (3.3)$$

Based on the relation

$$\mathcal{V}_W(T, \mu_B; \bar{\sigma}, \bar{\omega}_0) = \frac{T}{V} \ln \mathcal{Z}_W, \quad (3.4)$$

the effective potential of Walecka model is given by

$$\begin{aligned} \mathcal{V}_W(T, \mu_B) = & -\frac{T}{V} \sum_n \int \frac{d^3\mathbf{k}}{(2\pi)^3} \sum_{N=n,p} \ln \det [\mathcal{S}_{0N}^{-1}(ik_n, \mathbf{k}) + \Sigma_N(\sigma, \omega_0)] \\ & + \frac{1}{2}m_\sigma^2\sigma^2 + U(\sigma) - \frac{1}{2}m_\omega^2\omega^\mu\omega_\mu, \end{aligned} \quad (3.5)$$

where  $\mathcal{S}_{0N}^{-1} = (ik_n + \mu_B)\gamma_0 - \boldsymbol{\gamma} \cdot \mathbf{k} - m_N$  is the inverse of the thermal Green's function of free nucleons, with  $k_n = (2n+1)\pi T$  ( $n \in \mathbb{Z}$ ). The quantities  $\Sigma_N$  are defined as  $\Sigma_n = \Sigma_p = g_\sigma\sigma - g_\omega\cancel{\omega}$ .

Because of the symmetry spontaneous breaking, the meson field can be decomposed into condensate and fluctuations, i.e  $\sigma = \bar{\sigma} + \delta\sigma$  and  $\omega^\mu = \bar{\omega}_0 + \delta\omega^\mu$ . In the MFA, the

fluctuations  $\delta\sigma$  and  $\delta\omega^\mu$  are neglected. At zero temperature, the equation of state in MFA of the Walecka model can be evaluated as

$$\bar{p}_W(\mu_B) = -\bar{\mathcal{V}}_W(\mu_B) = 2p_0(\mu_B^*, m_N^*) - \frac{1}{2}m_\sigma^2\bar{\sigma}^2 - U(\bar{\sigma}) + \frac{1}{2}m_\omega^2\bar{\omega}_0^2, \quad (3.6)$$

where the effective masses of quasi-nucleon  $m_N^*$  and quasi-Fermi surface  $\mu_B^*$  are

$$m_N^* = m_N - g_\sigma\bar{\sigma}, \quad (3.7a)$$

$$\mu_B^* = \mu_B - g_\omega\bar{\omega}_0. \quad (3.7b)$$

Note that the radiative correction from the vacuum contribution has been neglected. The meson condensates  $\bar{\sigma}$  and  $\bar{\omega}_0$  are determined by the following gap equations based on Eqs. (2.26):

$$-m_\omega^2\bar{\omega}_0 + 2g_\omega n_0(\mu_B^*, m_N^*) = 0, \quad (3.8a)$$

$$m_\sigma^2\bar{\sigma} + U'(\bar{\sigma}) - 2g_\sigma n_s(\mu_B^*, m_N^*) = 0. \quad (3.8b)$$

Here,  $n_s(\mu, m)$  is for the free scalar density defined as

$$n_s(\mu, m) = \frac{m}{2\pi^2} \left[ |\mu| \sqrt{\mu^2 - m^2} - m^2 \cosh^{-1} \left( \frac{|\mu|}{m} \right) \right] \Theta(|\mu| - m). \quad (3.9)$$

In our calculations, we set the model parameters as follows: The particle masses are taken to be  $m_N = 0.939$  GeV,  $m_\sigma = 0.550$  GeV, and  $m_\omega = 0.783$  GeV [82]. The coupling constants are chosen as  $g_\sigma^2/(4\pi) = 6.003$ ,  $g_\omega^2/(4\pi) = 5.948$ ,  $b = 7.950 \times 10^{-3}$ , and  $c = 6.952 \times 10^{-4}$  to fit the empirically known properties of nuclear matter [81]. To find all solutions of the gap equations, we apply the homotopy method to solve this nonlinear equation group [83, 84]. The static properties of nucleons at  $T = 0$  are shown in Figure 3. In

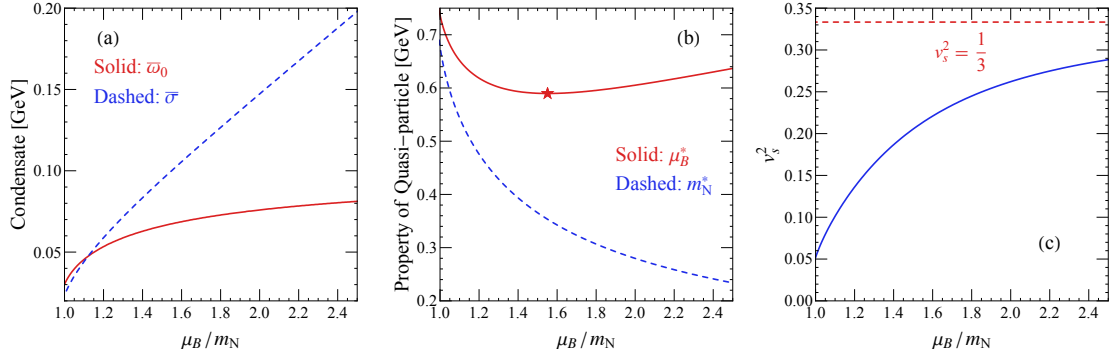


**Figure 3.** Static properties of nucleon matter depicted by the Walecka model presented as functions of  $\mu_B/m_N$ : (a)  $\bar{\omega}_0$  (red, solid) and  $\bar{\sigma}$  (blue, dashed); (b)  $\mu_B^*$  (red, solid) and  $m_N^*$  (blue, dashed), where the red star indicates the inflection point of  $\mu_B^*$ ; (c) squared sound velocity  $v_s^2$  (blue, solid) compared to the benchmark  $v_s^2 = 1/3$  (red, dashed).

Figure 3(b), as the density increases, an inflection point in  $\mu_B^*$  appears, i.e.,  $d\mu_B^*/d\mu_B = 0$ , marked by a red star. This will lead to a divergence at  $\mu_B \approx 1.551m_N$  in the derivative

$$\frac{dm_N^*}{d\mu_B^*} = -\frac{2g_\sigma^2 m_N^* p_F^*}{g_\sigma^2 \mu_B^* p_F^* + \pi^2 [m_\sigma^2 + U''(\bar{\sigma})] - 3g_\sigma^2 m_N^{*2} \cosh^{-1}(\mu_B^*/m_N^*)}, \quad (3.10)$$

which is calculated from Eq. (2.31). This divergence occurs because, although the Walecka model in the MFA can characterize the gas-liquid phase transition of nucleon matter, the ground state is not stable. The elements of the Hessian matrix are

$$\frac{\partial^2 \bar{\mathcal{V}}_W}{\partial \bar{\sigma}^2} = U''(\bar{\sigma}) + \frac{g_\sigma^2 \left[ \mu_B^* p_F^* - 3m_N^{*2} \cosh^{-1} \left( \frac{\mu_B^*}{m_N^*} \right) \right]}{\pi^2} + m_\sigma^2, \quad (3.11a)$$

$$\frac{\partial^2 \bar{\mathcal{V}}_W}{\partial \bar{\omega}^2} = -\frac{2g_\omega^2 \mu_B^* p_F^*}{\pi^2} - m_\omega^2, \quad (3.11b)$$

$$\frac{\partial^2 \bar{\mathcal{V}}_W}{\partial \bar{\omega} \partial \bar{\sigma}} = \frac{\partial^2 \bar{\mathcal{V}}_W}{\partial \bar{\sigma} \partial \bar{\omega}} = \frac{2g_\sigma g_\omega m_N^* p_F^*}{\pi^2}. \quad (3.11c)$$

Apparently,  $\partial^2 \bar{\mathcal{V}}_W / \partial \bar{\omega}^2$  in Eq. (3.11b) is always negative, while the off-diagonal elements in Eq. (3.11c) are positive. In Eq. (3.11a) we have

$$\lim_{\mu_B^*/m_N^* \rightarrow +\infty} \frac{\partial^2 \bar{\mathcal{V}}_W}{\partial \bar{\sigma}^2} > 0, \quad (3.12)$$

yet the Hessian matrix in Eq. (2.27a) cannot be guaranteed to be positive-definite. Therefore, even though the gap equations are solved, the stability condition specified by Eqs. (2.27) is not satisfied when  $\mu_N^*/m_N^* \gg 1$ . This suggests that the Walecka model, though widely used for the study of equilibrium properties of the nuclear matter, may not be suitable for the study of the dynamics properties, where the system can be driven out of local equilibrium.

### 3.2 Transport coefficients

Since the contribution of the one-pion exchange potential to the bulk properties of nuclear matter largely averages to zero [57, 85], we consider only the exchange of the  $\sigma$  and  $\omega$  mesons within the framework of the Walecka model. In the MFA, the system is treated as a free fermion gas, with part of the non-perturbative interaction effects incorporated into the effective mass  $m_N^*$  and effective chemical potential  $\mu_B^*$ . However, in such an MFA picture, scattering processes are absent. Therefore, we need to go beyond the MFA.

In Eq. (3.1a), the fermionic Lagrangian density can be decomposed as  $\mathcal{L}_f = \bar{\mathcal{L}}_f + \delta\mathcal{L}_f$ , where the MFA component is given by

$$\bar{\mathcal{L}}_f = \sum_{N=n,p} \bar{\psi}_N^* (i\cancel{\partial} - m_N^* + \mu_B^* \gamma^0) \psi_N^*, \quad (3.13)$$

and the interactions beyond the MFA are contained in the term

$$\delta\mathcal{L}_f = \sum_{N=n,p} \bar{\psi}_N^* (g_\sigma \delta\sigma - g_\omega \delta\psi) \psi_N^*. \quad (3.14)$$

Here,  $\psi_N^*$  denotes the spinor for quasi-particles characterized by  $m_N^*$  and  $\mu_B^*$ . The meson fluctuation fields  $\delta\sigma$  and  $\delta\omega^\mu$  follow the same dynamics described in  $\mathcal{L}_{\text{int}}$ . It is both interesting and crucial to examine the linear fluctuation terms in the mesonic sector. The gap equations, as presented in Eqs. (3.8), yield the following expressions<sup>6</sup>

$$m_\omega^2 \bar{\omega}_0 \delta\omega_0 = 2g_\omega \langle \psi_N^{*\dagger} \psi_N^* \rangle \delta\omega_0, \quad (3.15a)$$

---

<sup>6</sup> $\langle \dots \rangle$  denotes the statistical average over the thermodynamic ensemble.

$$m_\sigma^2 \bar{\sigma} \delta\sigma + U'(\bar{\sigma}) \delta\sigma = 2g_\sigma \langle \bar{\psi}_N^* \psi_N^* \rangle \delta\sigma. \quad (3.15b)$$

Here, we have used the definitions  $n_0 \equiv \langle \psi_N^{*\dagger} \psi_N^* \rangle$  and  $n_s \equiv \langle \bar{\psi}_N^* \psi_N^* \rangle$ . Notably, Eqs. (3.15) introduces the counterterms necessary to cancel the self-energy contributions in forward scattering. Neglecting fluctuations beyond the quadratic terms of mesonic fields, the self-energy corrections in the potential  $U(\sigma)$  modify the scalar meson mass from  $m_\sigma$  to

$$\tilde{m}_\sigma = \sqrt{m_\sigma^2 + 2bg_\sigma^3 m_N \bar{\sigma} + 4cg_\sigma^4 \bar{\sigma}^2}. \quad (3.16)$$

In this work, we consider only the leading-order scattering, i.e.,  $2 \leftrightarrow 2$  tree-level processes [66]. Therefore, only the  $t$  and  $u$  channels are present, as illustrated in Figure 4<sup>7</sup>. The total scattering amplitude is given by

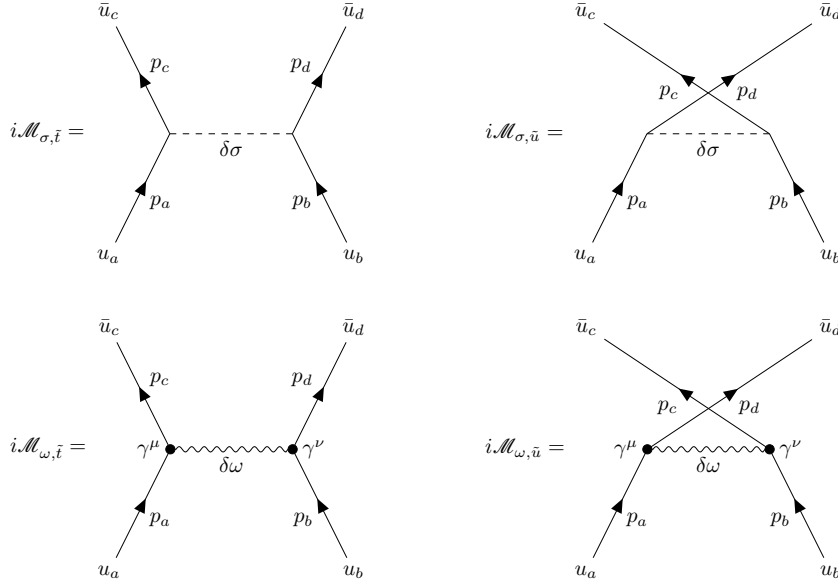


**Figure 4.** Feynman diagrams of leading-order nucleon-nucleon scattering including the exchange of the fluctuations of  $\sigma$  meson (upper panel) and the  $\omega$  meson (lower panel). Only the  $t$ -channel (left panel) and  $u$ -channel (right panel) contribute. The incoming and outgoing nucleons with four-momentum  $p_i$  ( $i = a, b, c, d$ ) are denoted by spinors  $u_i = u(p_i)$  and  $\bar{u}_i = \bar{u}(p_i)$ , respectively.

$$i\mathcal{M} = i \left[ \left( \mathcal{M}_{\sigma, \tilde{t}} - \mathcal{M}_{\sigma, \tilde{u}} \right) + \left( \mathcal{M}_{\omega, \tilde{t}} - \mathcal{M}_{\omega, \tilde{u}} \right) \right], \quad (3.17)$$

where the elements of the squared scattering amplitude are presented in Appendix B.

With this scattering amplitude, we can estimate the relaxation time  $\tau_{\text{rel}}$ . Considering that the binding energy of nucleons in heavy nuclei is around 8–10 MeV [86], we set the temperature to  $T = 8$  MeV to avoid thermal excitation. The scaled relaxation time is shown in Figure 5, where the relaxation time is fitted as

$$\tau_{\text{rel}}(x) = \frac{755x^4 - 564x^3 - 80.9x^2 + 74.4x + 3.95}{x^5 - 0.459x^4 - 0.631x^2}, \quad x = \frac{\mu_B^*}{m_N^*} > 1. \quad (3.18)$$

<sup>7</sup>To avoid repeating labels, we represent the Mandelstam variables using  $\tilde{\sigma}$ , where  $\sigma = s, t, u$ .

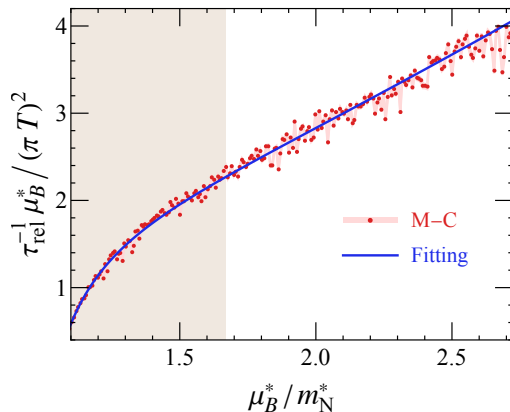


**Figure 5.** The scaled relaxation time  $\tau_{\text{rel}}^{-1} \mu_B^* / (\pi T)^2$  as a function of  $\mu_B^* / m_N^*$ . The red band is calculated from Monte Carlo (M-C) integration [87]. The blue solid line is a fit to the M-C data given in Eq. (3.18). The brown shaded area indicates the physical region predicted by the Walecka model.

As in the discussion of Eqs. (3.11), the physical region (brown shaded area in Figure 5) depicted by the Walecka model is defined as the region where the transport coefficients are positive. In this physical region, the relaxation time of dense and cold nucleon matter is of the order  $\mu_B^* / (\pi T)^2$ . At low density, i.e., small  $\mu_B$ , the relaxation time is large because the collision integral over phase space becomes zero if nucleon-bound states are not formed. Under this condition, the relaxation time diverges to infinity. As the density increases, the mean free path reduces gradually, resulting in more frequent collisions within a given time period; therefore, the relaxation time decreases.

At finite baryon density, the fluidity of the system should be assessed based on the ratio of the transport coefficients to the enthalpy [88, 89]. In the MFA at  $T = 0$ <sup>8</sup>, the energy density is evaluated as

$$\bar{\varepsilon}_W(\mu_B^*, m_N^*) = 2\varepsilon_0(\mu_B^*, m_N^*) + \frac{1}{2}m_\sigma^2 \bar{\sigma}^2 + U(\bar{\sigma}) + \frac{1}{2}m_\omega^2 \bar{\omega}_0^2, \quad (3.19)$$

and the enthalpy density is calculated as

$$\bar{h}_W(\mu_B^*, m_N^*) = \bar{p}_W(\mu_B^*, m_N^*) + \bar{\varepsilon}_W(\mu_B^*, m_N^*). \quad (3.20)$$

The dimensionless enthalpy-scaled shear viscosity and bulk viscosity are shown in Figure 6. In Figure 6(a), the scaled shear viscosity always decreases with increasing density, even beyond the physical region. The shear viscosity measures the resistance of fluid to shear flow. At higher densities, interactions among particles may facilitate easier sliding past one another because of the decreasing mean free path, reducing the shear viscosity. In contrast, the bulk viscosity in Figure 6(b) is non-monotonic even within the physical region. This is because the bulk viscosity depends not only on microscopic interactions but also on complex

<sup>8</sup>We consider the condition  $T/\mu_B^* \ll 1$ , where both the static properties and the thermodynamic quantities at  $T = 0$  serve as a good approximation at leading order expansion of  $f_0$ .



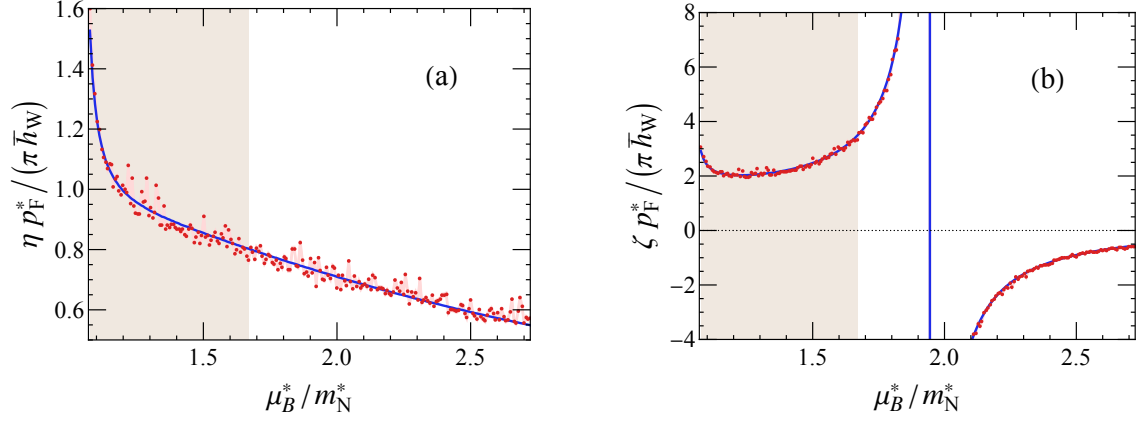


**Figure 6.** The dimensionless scaled (a) shear viscosity  $\eta p_{\text{F}}^*/(\pi \bar{h}_{\text{W}})$  and (b) bulk viscosity  $\zeta p_{\text{F}}^*/(\pi \bar{h}_{\text{W}})$  as functions of  $\mu_{\text{B}}^*/m_{\text{N}}^*$ . The labels are the same to Figure 5.

static thermodynamic properties reflected in the derivative terms in Eq. (2.32b). Both the divergence and the negative values of the bulk viscosity in the nonphysical region result from the instability of the Walecka model, as mentioned in Eqs. (3.11). We also notice that the bulk viscosity is nearly twice the shear viscosity. This suggests that in the cold and dense nucleon matter, processes involving compression or expansion are more heavily damped than those involving shear, indicating stronger interactions or relaxation processes that specifically resist volumetric deformation. The mechanisms for dissipating energy are more effective when dealing with changes in volume rather than shape.

## 4 Conclusion and outlook

In this work, we employed the Boltzmann equation framework within the Fermi liquid picture to investigate the transport properties of dense matter at extremely low temperatures. At leading order in the gradient expansion of the particle distribution function, we observed that fluctuations are primarily concentrated near the Fermi surface. Utilizing the RTA, we derived general expressions for both shear and bulk viscosities.

The static properties of nucleon matter were described using the Walecka model in the mean-field approximation. Our findings indicate that, at leading order in scattering, the relaxation time scales as  $\tau_{\text{rel}} \sim \mu_{\text{B}}^*/(\pi T)^2$ . The fluidity of the cold and dense nucleon matter is characterized through shear and bulk viscosities of the order  $p_{\text{F}}^*/(\pi \bar{h}_{\text{W}})$ . Notably, the bulk viscosity is approximately twice the shear viscosity, suggesting that dissipation in the system more readily occurs through volumetric deformation rather than shear processes.

During the formulation of the transport coefficients, we observed that an isotropic Fermi surface at zero temperature prohibits collisions because all states below the Fermi energy are occupied, leaving no available states for fermions to scatter into above the Fermi surface. To address this, we introduced a negligible temperature to slightly deform the Fermi surface, enabling collisions. Fortunately, such deformation naturally occurs in nucleon matter due to

spin polarization [90, 91] and in neutron stars where magnetic fields affect the nucleons [92], where the transport coefficients at exact zero temperature can be studied.

Moreover, as we have pointed out, the Walecka model possesses inherent instabilities. To accurately describe nucleons and their interactions, more detailed calculations based on nucleon-nucleon scattering are necessary [93, 94]. Additionally, since the nuclei system is of finite size, the clear separation of length scales required for hydrodynamics may be absent. To study energy dissipation in such systems, it is essential to investigate response regimes beyond hydrodynamics [95–98].

Beyond nuclear physics, due to the artificially controlled scattering length in Feshbach resonance experiments, the transport coefficients in finite-size systems can also be examined in cold fermion atom systems [99, 100]. These avenues offer promising directions for future research into the transport properties of dense fermionic systems.

## 5 Acknowledgment

The authors express gratitude for the valuable discussions and comments from Lipei Du, Defu Hou, Jin Hu, Fabian Rennecke, Andrey Sadofyev, Shuzhe Shi and Yi Yin. J. L. is supported by funding from project No. 2004HBBHJD054.

## A Collision term

In this appendix, we present the detailed calculation of the collision term. Based on Eq. (2.40), we separate  $\omega(E_a^*)$  in Eq. (2.37) into

$$\omega(E_a^*) = -\omega_{cd\delta b} + \omega_{d\bar{b}\delta c} + \omega_{c\bar{b}\delta d}. \quad (\text{A.1})$$

Throughout this calculation, we set  $\mathbf{p}_a$  along the  $z$ -direction, i.e.,

$$p_a^\mu = (E_a^*, 0, 0, |\mathbf{p}_a|). \quad (\text{A.2})$$

In the local rest frame of the fluid cell, the first term contributing to  $\omega(E_a^*)$  is calculated as<sup>9</sup>

$$\omega_{cd\delta b} = \frac{(\pi T)^2}{24p_F^*} \frac{d}{d|\mathbf{p}_b|} \mathcal{F}_1(|\mathbf{p}_a|, |\hat{\mathbf{p}}_c|, \Omega_b, \Omega_c) \Big|_{\substack{|\mathbf{p}_b|=p_F^* \\ E_a^*=\mu^*}}, \quad (\text{A.3})$$

where

$$\mathcal{F}_1(|\mathbf{p}_a|, |\hat{\mathbf{p}}_c|, \Omega_b, \Omega_c) = \iint d\Omega_b d\Omega_c \frac{|\mathbf{p}_b| |\hat{\mathbf{p}}_c|}{32\hat{E}_d^* (2\pi)^5} |\mathcal{M}|^2 \Theta(\mu^* - \hat{E}_c^*) \Theta(\mu^* - \hat{E}_d^*). \quad (\text{A.4})$$

Here, we introduce a new notation

$$\hat{E}_i^* = \sqrt{\hat{\mathbf{p}}_i^2 + m^2}. \quad (\text{A.5})$$

---

<sup>9</sup>The hat symbol ( $\hat{\cdot}$ ) indicates that the variable ( $\varphi$ ) should be expressed as a function of other independent variables.

Generally, in this section,  $\Omega_i$  represents the solid angle between the  $i$ th momentum to  $z$ -direction. The other two four-momenta are defined as

$$\mathbf{p}_b^\mu = (E_b^*, |\mathbf{p}_b| \sin \theta_b \cos \phi_b, |\mathbf{p}_b| \sin \theta_b \sin \phi_b, |\mathbf{p}_b| \cos \theta_b), \quad (\text{A.6a})$$

$$\hat{\mathbf{p}}_c^\mu = \left( \hat{E}_c^*, |\hat{\mathbf{p}}_c| \sin \theta_c \cos \phi_c, |\hat{\mathbf{p}}_c| \sin \theta_c \sin \phi_c, |\hat{\mathbf{p}}_c| \cos \theta_c \right). \quad (\text{A.6b})$$

By solving the equation

$$\tilde{s} + 2 |\hat{\mathbf{p}}_c| |\mathbf{p}_{a+b}| \cos \hat{\theta}_{a+b}^c = 2E_{a+b}^* \sqrt{\hat{\mathbf{p}}_c^2 + m^{*2}}, \quad (\text{A.7})$$

we obtain<sup>10</sup>

$$|\hat{\mathbf{p}}_c| = \frac{|\mathbf{p}_{a+b}| \tilde{s} \cos \hat{\theta}_{a+b}^c + E_{a+b}^* \sqrt{2m^{*2} (\mathbf{p}_{a+b}^2 - 2E_{a+b}^{*2}) + 2m^{*2} \mathbf{p}_{a+b}^2 \cos 2\hat{\theta}_{a+b}^c + \tilde{s}^2}}{2 \left( E_{a+b}^{*2} - \mathbf{p}_{a+b}^2 \cos^2 \hat{\theta}_{a+b}^c \right)}, \quad (\text{A.8})$$

with

$$\tilde{s} = (p_a + p_b)^2, \quad (\text{A.9a})$$

$$E_{a+b}^* = E_a^* + E_b^*, \quad (\text{A.9b})$$

$$|\mathbf{p}_{a+b}| = |\mathbf{p}_a + \mathbf{p}_b| = \sqrt{\mathbf{p}_a^2 + \mathbf{p}_b^2 + 2 |\mathbf{p}_a| |\mathbf{p}_b| \cos \theta_b}, \quad (\text{A.9c})$$

$$\hat{\theta}_{a+b}^c = \cos^{-1} \left[ \frac{\cos \theta_c (|\mathbf{p}_b| \cos \theta_b + |\mathbf{p}_a|) + |\mathbf{p}_b| \sin \theta_b \sin \theta_c \cos (\phi_b - \phi_c)}{|\mathbf{p}_{a+b}|} \right]. \quad (\text{A.9d})$$

To compute Eq. (A.4), we use the relation

$$|\hat{\mathbf{p}}_d| = \sqrt{E_{a+b}^* \left( E_{a+b}^* - 2\hat{E}_c^* \right) + \hat{\mathbf{p}}_c^2}. \quad (\text{A.10})$$

Here,  $\theta_i$  and  $\phi_i$  are the polar and azimuthal angles, respectively, and  $\hat{\theta}_i^j$  represents the polar angle between  $i$ th and the  $j$ th momentum. Although the subscripts may change in the following calculations, their physical meanings remain the same, and we will not clarify them again.

Similarly, the second part can be calculated as

$$\omega_{d\bar{b}\delta c} = \frac{(\pi T)^2}{24p_F^*} \frac{d}{d|\mathbf{p}_c|} \mathcal{F}_2(|\mathbf{p}_a|, |\mathbf{p}_c|, \Omega_b, \Omega_c) \Big|_{\substack{|\mathbf{p}_c|=p_F^* \\ E_a^*=\mu^*}}, \quad (\text{A.11})$$

with

$$\mathcal{F}_2(|\mathbf{p}_a|, |\mathbf{p}_c|, \Omega_b, \Omega_c) = \iint d\Omega_b d\Omega_c \frac{|\hat{\mathbf{p}}_b| |\mathbf{p}_c|}{32\hat{E}_d^* (2\pi)^5} |\mathcal{M}|^2 \Theta(\mu^* - \hat{E}_d^*) \Theta(\hat{E}_b^* - \mu^*). \quad (\text{A.12})$$

With

$$\hat{\mathbf{p}}_b^\mu = \left( \hat{E}_b^*, |\hat{\mathbf{p}}_b| \sin \theta_b \cos \phi_b, |\hat{\mathbf{p}}_b| \sin \theta_b \sin \phi_b, |\hat{\mathbf{p}}_b| \cos \theta_b \right), \quad (\text{A.13a})$$

<sup>10</sup>The redundant solution for  $|\hat{\mathbf{p}}_c|$  is discarded based on the condition  $|\hat{\mathbf{p}}_c| > 0$ .

$$p_c^\mu = (E_c^*, |\mathbf{p}_c| \sin \theta_c \cos \phi_c, |\mathbf{p}_c| \sin \theta_c \sin \phi_c, |\mathbf{p}_c| \cos \theta_c), \quad (\text{A.13b})$$

and by solving the equation

$$\tilde{t} + 2 |\hat{\mathbf{p}}_b| |\mathbf{p}_{c-a}| \cos \hat{\theta}_{c-a}^b = 2E_{c-a}^* \sqrt{\mathbf{p}_b^2 + m^{*2}}, \quad (\text{A.14})$$

other variables are expressed as

$$|\hat{\mathbf{p}}_b| = \frac{|\mathbf{p}_{c-a}| \tilde{t} \cos \hat{\theta}_{c-a}^b - E_{c-a}^* \sqrt{2m^{*2} (\mathbf{p}_{c-a}^2 - 2E_{c-a}^{*2}) + 2m^{*2} \mathbf{p}_{c-a}^2 \cos 2\hat{\theta}_{c-a}^b + \tilde{t}^2}}{2 (E_{c-a}^{*2} - \mathbf{p}_{c-a}^2 \cos^2 \hat{\theta}_{c-a}^b)}, \quad (\text{A.15})$$

and

$$\tilde{t} = (p_c - p_a)^2, \quad (\text{A.16a})$$

$$E_{c-a}^* = E_c^* - E_a^*, \quad (\text{A.16b})$$

$$|\mathbf{p}_{c-a}| = |\mathbf{p}_c - \mathbf{p}_a| = \sqrt{\mathbf{p}_a^2 + \mathbf{p}_c^2 - 2|\mathbf{p}_a| |\mathbf{p}_c| \cos \theta_c} \quad (\text{A.16c})$$

$$\hat{\theta}_{c-a}^b = \cos^{-1} \left[ \frac{\cos \theta_b (|\mathbf{p}_c| \cos \theta_c - |\mathbf{p}_a|) + |\mathbf{p}_c| \sin \theta_b \sin \theta_c \cos (\phi_b - \phi_c)}{|\mathbf{p}_{c-a}|} \right]. \quad (\text{A.16d})$$

Moreover, we have

$$|\hat{\mathbf{p}}_d| = \sqrt{E_{c-a}^* (E_{c-a}^* - 2\hat{E}_b^*) + \hat{\mathbf{p}}_b^2}. \quad (\text{A.17})$$

The third part is calculated as

$$\omega_{c\hat{b}\delta d} = \frac{(\pi T)^2}{24 p_F^*} \frac{d}{d|\mathbf{p}_d|} \mathcal{F}_3(|\mathbf{p}_a|, |\mathbf{p}_d|, \Omega_b, \Omega_d) \Big|_{\substack{|\mathbf{p}_d|=p_F^* \\ E_a^*=\mu^*}}, \quad (\text{A.18})$$

with

$$\mathcal{F}_3(|\mathbf{p}_a|, |\mathbf{p}_d|, \Omega_b, \Omega_d) = \iint d\Omega_b d\Omega_d \frac{|\hat{\mathbf{p}}_b| |\mathbf{p}_d|}{32 \hat{E}_c^* (2\pi)^5} |\mathcal{M}|^2 \Theta(\mu^* - \hat{E}_c^*) \Theta(\hat{E}_b^* - \mu^*). \quad (\text{A.19})$$

With the independent momenta written as

$$\hat{p}_b^\mu = (\hat{E}_b^*, |\hat{\mathbf{p}}_b| \sin \theta_b \cos \phi_b, |\hat{\mathbf{p}}_b| \sin \theta_b \sin \phi_b, |\hat{\mathbf{p}}_b| \cos \theta_b), \quad (\text{A.20a})$$

$$p_d^\mu = (E_d^*, |\mathbf{p}_d| \sin \theta_d \cos \phi_d, |\mathbf{p}_d| \sin \theta_d \sin \phi_d, |\mathbf{p}_d| \cos \theta_d), \quad (\text{A.20b})$$

and by solving the equation

$$\tilde{u} + 2 |\hat{\mathbf{p}}_b| |\mathbf{p}_{d-a}| \cos \hat{\theta}_{d-a}^b = 2E_{d-a}^* \sqrt{\mathbf{p}_b^2 + m^{*2}}, \quad (\text{A.21})$$

other variables are expressed as

$$|\hat{\mathbf{p}}_b| = \frac{|\mathbf{p}_{d-a}| \tilde{u} \cos \hat{\theta}_{d-a}^b - E_{d-a}^* \sqrt{2m^{*2} (\mathbf{p}_{d-a}^2 - 2E_{d-a}^{*2}) + 2m^{*2} \mathbf{p}_{d-a}^2 \cos 2\hat{\theta}_{d-a}^b + \tilde{u}^2}}{2 (E_{d-a}^{*2} - \mathbf{p}_{d-a}^2 \cos^2 \hat{\theta}_{d-a}^b)}, \quad (\text{A.22a})$$

$$\tilde{u} = (p_d - p_a)^2, \quad (\text{A.22b})$$

$$E_{d-a}^* = E_d^* - E_a^*, \quad (\text{A.22c})$$

$$|\mathbf{p}_{d-a}| = |\mathbf{p}_d - \mathbf{p}_a| = \sqrt{\hat{\mathbf{p}}_d^2 + \hat{\mathbf{p}}_a^2 - 2|\hat{\mathbf{p}}_a||\hat{\mathbf{p}}_d|\cos\theta_d} \quad (\text{A.22d})$$

$$\hat{\theta}_{d-a}^b = \cos^{-1} \left[ \frac{\cos\theta_b (|\mathbf{p}_d| \cos\theta_d - |\mathbf{p}_a|) + |\mathbf{p}_d| \sin\theta_b \sin\theta_d \cos(\phi_d - \phi_b)}{|\mathbf{p}_{d-a}|} \right]. \quad (\text{A.22e})$$

and also

$$|\hat{\mathbf{p}}_c| = \sqrt{E_{d-a}^* (E_{d-a}^* - 2\hat{E}_b^*) + \hat{\mathbf{p}}_b^2}. \quad (\text{A.23})$$

## B Calculation of the squared scattering amplitude

Using FEYNCalc 9.3.1 [101–103], the elements in  $\sum_{\text{spins}} |\mathcal{M}|^2$  are calculated as

$$\sum_{\text{spins}} |\mathcal{M}_{\sigma, \tilde{t}}|^2 = \frac{4g_\sigma^4}{(\tilde{t} - \tilde{m}_\sigma^2)^2} (\tilde{t} - 4m_N^{*2})^2, \quad (\text{B.1a})$$

$$\sum_{\text{spins}} |\mathcal{M}_{\sigma, \tilde{u}}|^2 = \frac{4g_\sigma^4}{(\tilde{u} - \tilde{m}_\sigma^2)^2} (\tilde{u} - 4m_N^{*2})^2, \quad (\text{B.1b})$$

$$\sum_{\text{spins}} |\mathcal{M}_{\omega, \tilde{t}}|^2 = \frac{4g_\omega^4}{(\tilde{t} - m_\omega^2)^2} \left[ (\tilde{s} + \tilde{t})^2 + (\tilde{t} + \tilde{u})^2 - (\tilde{s} + \tilde{u})^2 + (\tilde{s}^2 + \tilde{t}^2 + \tilde{u}^2) \right], \quad (\text{B.1c})$$

$$\sum_{\text{spins}} |\mathcal{M}_{\omega, \tilde{u}}|^2 = \frac{4g_\omega^4}{(\tilde{u} - m_\omega^2)^2} \left[ (\tilde{s} + \tilde{u})^2 + (\tilde{t} + \tilde{u})^2 - (\tilde{s} + \tilde{t})^2 + (\tilde{s}^2 + \tilde{t}^2 + \tilde{u}^2) \right], \quad (\text{B.1d})$$

$$\sum_{\text{spins}} \Re(\mathcal{M}_{\sigma, \tilde{t}} \mathcal{M}_{\sigma, \tilde{u}}^*) = \frac{g_\sigma^4}{(\tilde{t} - \tilde{m}_\sigma^2)(\tilde{u} - \tilde{m}_\sigma^2)} \left[ (\tilde{s} + \tilde{t})^2 + (\tilde{s} + \tilde{u})^2 - (\tilde{t} + \tilde{u})^2 \right], \quad (\text{B.1e})$$

$$\sum_{\text{spins}} \Re(\mathcal{M}_{\omega, \tilde{t}} \mathcal{M}_{\omega, \tilde{u}}^*) = \frac{2g_\omega^4}{(\tilde{t} - m_\omega^2)(\tilde{u} - m_\omega^2)} \left[ (\tilde{s} + \tilde{t})^2 + (\tilde{s} + \tilde{u})^2 - 3(\tilde{t} + \tilde{u})^2 - (\tilde{s}^2 + \tilde{t}^2 + \tilde{u}^2) \right], \quad (\text{B.1f})$$

$$\sum_{\text{spins}} \Re(\mathcal{M}_{\sigma, \tilde{t}} \mathcal{M}_{\omega, \tilde{t}}^*) = -\frac{16g_\sigma^2 g_\omega^2}{(\tilde{t} - \tilde{m}_\sigma^2)(\tilde{t} - m_\omega^2)} m_N^{*2} (\tilde{s} - \tilde{u}), \quad (\text{B.1g})$$

$$\sum_{\text{spins}} \Re(\mathcal{M}_{\sigma, \tilde{u}} \mathcal{M}_{\omega, \tilde{u}}^*) = -\frac{16g_\sigma^2 g_\omega^2}{(\tilde{u} - \tilde{m}_\sigma^2)(\tilde{u} - m_\omega^2)} m_N^{*2} (\tilde{s} - \tilde{t}), \quad (\text{B.1h})$$

$$\sum_{\text{spins}} \Re(\mathcal{M}_{\sigma, \tilde{t}} \mathcal{M}_{\omega, \tilde{u}}^*) = -\frac{g_\sigma^2 g_\omega^2}{(\tilde{t} - \tilde{m}_\sigma^2)(\tilde{u} - m_\omega^2)} \left[ 4(\tilde{s} + \tilde{u})^2 + (\tilde{t} + \tilde{u})^2 - (\tilde{s} + \tilde{t})^2 + \tilde{u}^2 - \tilde{s}^2 \right], \quad (\text{B.1i})$$

$$\sum_{\text{spins}} \Re(\mathcal{M}_{\sigma, \tilde{u}} \mathcal{M}_{\omega, \tilde{t}}^*) = -\frac{g_\sigma^2 g_\omega^2}{(\tilde{u} - \tilde{m}_\sigma^2)(\tilde{t} - m_\omega^2)} \left[ 4(\tilde{s} + \tilde{t})^2 + (\tilde{t} + \tilde{u})^2 - (\tilde{s} + \tilde{u})^2 + \tilde{t}^2 - \tilde{s}^2 \right]. \quad (\text{B.1j})$$

## References

- [1] A. Andronic et al., *Hadron Production in Ultra-relativistic Nuclear Collisions: Quarkyonic Matter and a Triple Point in the Phase Diagram of QCD*, *Nucl. Phys. A* **837** (2010) 65 [[0911.4806](#)].
- [2] U. Heinz and R. Snellings, *Collective flow and viscosity in relativistic heavy-ion collisions*, *Ann. Rev. Nucl. Part. Sci.* **63** (2013) 123 [[1301.2826](#)].
- [3] E. Shuryak, *Strongly coupled quark-gluon plasma in heavy ion collisions*, *Rev. Mod. Phys.* **89** (2017) 035001 [[1412.8393](#)].
- [4] W. Busza, K. Rajagopal and W. van der Schee, *Heavy Ion Collisions: The Big Picture, and the Big Questions*, *Ann. Rev. Nucl. Part. Sci.* **68** (2018) 339 [[1802.04801](#)].
- [5] H. Song and U.W. Heinz, *Causal viscous hydrodynamics in 2+1 dimensions for relativistic heavy-ion collisions*, *Phys. Rev. C* **77** (2008) 064901 [[0712.3715](#)].
- [6] M. Luzum and P. Romatschke, *Conformal relativistic viscous hydrodynamics: Applications to RHIC results at  $\sqrt{s_{NN}} = 200$  GeV*, *Phys. Rev. C* **78** (2008) 034915 [[0804.4015](#)].
- [7] B. Schenke, S. Jeon and C. Gale, *(3+1)D hydrodynamic simulation of relativistic heavy-ion collisions*, *Phys. Rev. C* **82** (2010) 014903 [[1004.1408](#)].
- [8] C. Gale, S. Jeon, B. Schenke, P. Tribedy and R. Venugopalan, *Event-by-event anisotropic flow in heavy-ion collisions from combined Yang-Mills and viscous fluid dynamics*, *Phys. Rev. Lett.* **110** (2013) 012302 [[1209.6330](#)].
- [9] L. Del Zanna, V. Chandra, G. Inghirami, V. Rolando, A. Beraudo, A. De Pace et al., *Relativistic viscous hydrodynamics for heavy-ion collisions with ECHO-QGP*, *Eur. Phys. J. C* **73** (2013) 2524 [[1305.7052](#)].
- [10] PHENIX collaboration, *Identified charged particle spectra and yields in Au + Au collisions at  $\sqrt{s_{NN}} = 200$  GeV*, *Phys. Rev. C* **69** (2004) 034909 [[nucl-ex/0307022](#)].
- [11] A. Bzdak, S. Esumi, V. Koch, J. Liao, M. Stephanov and N. Xu, *Mapping the Phases of Quantum Chromodynamics with Beam Energy Scan*, *Phys. Rept.* **853** (2020) 1 [[1906.00936](#)].
- [12] X. An et al., *The BEST framework for the search for the QCD critical point and the chiral magnetic effect*, *Nucl. Phys. A* **1017** (2022) 122343 [[2108.13867](#)].
- [13] B. Muller, J. Schukraft and B. Wyslouch, *First Results from Pb+Pb collisions at the LHC*, *Ann. Rev. Nucl. Part. Sci.* **62** (2012) 361 [[1202.3233](#)].
- [14] ALICE collaboration, *Anisotropic flow of charged particles in Pb-Pb collisions at  $\sqrt{s_{NN}} = 5.02$  TeV*, *Phys. Rev. Lett.* **116** (2016) 132302 [[1602.01119](#)].
- [15] ALICE collaboration, *Energy dependence and fluctuations of anisotropic flow in Pb-Pb collisions at  $\sqrt{s_{NN}} = 5.02$  and 2.76 TeV*, *JHEP* **07** (2018) 103 [[1804.02944](#)].
- [16] N. Andersson and K.D. Kokkotas, *Towards gravitational wave asteroseismology*, *Mon. Not. Roy. Astron. Soc.* **299** (1998) 1059 [[gr-qc/9711088](#)].
- [17] P. Haensel, A.Y. Potekhin and D.G. Yakovlev, *Neutron stars 1: Equation of state and structure*, vol. 326, Springer, New York, USA (2007).
- [18] K.A. Van Riper, *Neutron star thermal evolution*, *Astrophysical Journal Supplement Series (ISSN 0067-0049)*, vol. 75, Feb. 1991, p. 449-462. DOE-supported research. **75** (1991) 449.

- [19] D.G. Yakovlev and C.J. Pethick, *Neutron star cooling*, *Ann. Rev. Astron. Astrophys.* **42** (2004) 169 [[astro-ph/0402143](#)].
- [20] D. Page, U. Geppert and F. Weber, *The Cooling of compact stars*, *Nucl. Phys. A* **777** (2006) 497 [[astro-ph/0508056](#)].
- [21] P. Goldreich and A. Reisenegger, *Magnetic field decay in isolated neutron stars*, *Astrophysical Journal, Part 1 (ISSN 0004-637X)*, vol. 395, no. 1, p. 250-258. **395** (1992) 250.
- [22] A.P. Igoshev, S.B. Popov and R. Hollerbach, *Evolution of Neutron Star Magnetic Fields*, *Universe* **7** (2021) 351 [[2109.05584](#)].
- [23] L. Lindblom, B.J. Owen and S.M. Morsink, *Gravitational radiation instability in hot young neutron stars*, *Phys. Rev. Lett.* **80** (1998) 4843 [[gr-qc/9803053](#)].
- [24] L. Lindblom and B.J. Owen, *Effect of hyperon bulk viscosity on neutron star r modes*, *Phys. Rev. D* **65** (2002) 063006 [[astro-ph/0110558](#)].
- [25] LIGO SCIENTIFIC, VIRGO collaboration, *GW170817: Observation of Gravitational Waves from a Binary Neutron Star Inspiral*, *Phys. Rev. Lett.* **119** (2017) 161101 [[1710.05832](#)].
- [26] B. Margalit and B.D. Metzger, *Constraining the Maximum Mass of Neutron Stars From Multi-Messenger Observations of GW170817*, *Astrophys. J. Lett.* **850** (2017) L19 [[1710.05938](#)].
- [27] E. Annala, T. Gorda, A. Kurkela, J. Nättilä and A. Vuorinen, *Evidence for quark-matter cores in massive neutron stars*, *Nature Phys.* **16** (2020) 907 [[1903.09121](#)].
- [28] L. Rezzolla and K. Takami, *Gravitational-wave signal from binary neutron stars: a systematic analysis of the spectral properties*, *Phys. Rev. D* **93** (2016) 124051 [[1604.00246](#)].
- [29] I. Bombaci and D. Logoteta, *Equation of state of dense nuclear matter and neutron star structure from nuclear chiral interactions*, *Astron. Astrophys.* **609** (2018) A128 [[1805.11846](#)].
- [30] T. Schäfer and D. Teaney, *Nearly Perfect Fluidity: From Cold Atomic Gases to Hot Quark Gluon Plasmas*, *Rept. Prog. Phys.* **72** (2009) 126001 [[0904.3107](#)].
- [31] P. Chakraborty and J.I. Kapusta, *Quasi-Particle Theory of Shear and Bulk Viscosities of Hadronic Matter*, *Phys. Rev. C* **83** (2011) 014906 [[1006.0257](#)].
- [32] M.G. Alford, H. Nishimura and A. Sedrakian, *Transport coefficients of two-flavor superconducting quark matter*, *Phys. Rev. C* **90** (2014) 055205 [[1408.4999](#)].
- [33] R.-A. Tripolt, *Spectral Functions and Transport Coefficients from the Functional Renormalization Group*, Ph.D. thesis, Darmstadt, Tech. Hochsch., 2015.
- [34] P. Deb, G.P. Kadam and H. Mishra, *Estimating transport coefficients in hot and dense quark matter*, *Phys. Rev. D* **94** (2016) 094002 [[1603.01952](#)].
- [35] JETSCAPE collaboration, *Multisystem Bayesian constraints on the transport coefficients of QCD matter*, *Phys. Rev. C* **103** (2021) 054904 [[2011.01430](#)].
- [36] J. Hu and S. Shi, *Multicomponent second-order dissipative relativistic hydrodynamics with binary reactive collisions*, *Phys. Rev. D* **106** (2022) 014007 [[2204.10100](#)].
- [37] P. Kovtun, D.T. Son and A.O. Starinets, *Viscosity in strongly interacting quantum field theories from black hole physics*, *Phys. Rev. Lett.* **94** (2005) 111601 [[hep-th/0405231](#)].

- [38] P. Achenbach et al., *The present and future of QCD*, *Nucl. Phys. A* **1047** (2024) 122874 [2303.02579].
- [39] V.E. Fortov, B.Y. Sharkov and H. Stoker, *European facility for antiproton and ion research (FAIR): The new international center for fundamental physics and its research program*, *Phys. Usp.* **55** (2012) 582.
- [40] NICA collaboration, *The nuclotron-based ion collider facility (NICA) at JINR: New prospects for heavy ion collisions and spin physics*, *J. Phys. G* **36** (2009) 064069.
- [41] HIAF PROJECT TEAM collaboration, *Status of the high-intensity heavy-ion accelerator facility in China*, *AAPPS Bull.* **32** (2022) 35.
- [42] P.A. Evans et al., *Swift and NuSTAR observations of GW170817: detection of a blue kilonova*, *Science* **358** (2017) 1565 [1710.05437].
- [43] B.P. Abbott et al., *Multi-messenger Observations of a Binary Neutron Star Merger*, *Astrophys. J. Lett.* **848** (2017) L12 [1710.05833].
- [44] J. Steinheimer and M. Bleicher, *Extraction of the sound velocity from rapidity spectra: Evidence for QGP formation at FAIR/RHIC-BES energies*, *Eur. Phys. J. A* **48** (2012) 100 [1207.2792].
- [45] V. Vovchenko, B. Dönigus and H. Stoecker, *Multiplicity dependence of light nuclei production at LHC energies in the canonical statistical model*, *Phys. Lett. B* **785** (2018) 171 [1808.05245].
- [46] M. Bleicher and E. Bratkovskaya, *Modelling relativistic heavy-ion collisions with dynamical transport approaches*, *Prog. Part. Nucl. Phys.* **122** (2022) 103920.
- [47] J. Li, L. Du and S. Shi, *Rapidity scan approach for net-baryon cumulants with a statistical thermal model*, *Phys. Rev. C* **109** (2024) 034906 [2311.11374].
- [48] A. Accardi et al., *Electron Ion Collider: The Next QCD Frontier: Understanding the glue that binds us all*, *Eur. Phys. J. A* **52** (2016) 268 [1212.1701].
- [49] D.P. Anderle et al., *Electron-ion collider in China*, *Front. Phys. (Beijing)* **16** (2021) 64701 [2102.09222].
- [50] J.J. Ethier and E.R. Nocera, *Parton Distributions in Nucleons and Nuclei*, *Ann. Rev. Nucl. Part. Sci.* **70** (2020) 43 [2001.07722].
- [51] R. Abdul Khalek et al., *Science Requirements and Detector Concepts for the Electron-Ion Collider: EIC Yellow Report*, *Nucl. Phys. A* **1026** (2022) 122447 [2103.05419].
- [52] C. Shen and B. Schenke, *Longitudinal dynamics and particle production in relativistic nuclear collisions*, *Phys. Rev. C* **105** (2022) 064905 [2203.04685].
- [53] W. Zhao, C. Shen and B. Schenke, *Collectivity in Ultraperipheral Pb+Pb Collisions at the Large Hadron Collider*, *Phys. Rev. Lett.* **129** (2022) 252302 [2203.06094].
- [54] B. Schenke, C. Shen and W. Zhao, *Collectivity in ultra-peripheral heavy-ion and e+A collisions*, in *Diffraction and Low-x 2024*, 11, 2024 [2411.18407].
- [55] X.-G. Deng, D.-Q. Fang and Y.-G. Ma, *Shear viscosity of nucleonic matter*, *Prog. Part. Nucl. Phys.* **136** (2024) 104095 [2401.02293].
- [56] G. Aarts, *Complex Langevin dynamics and other approaches at finite chemical potential*, *PoS LATTICE2012* (2012) 017 [1302.3028].



- [57] J.D. Walecka, *A Theory of highly condensed matter*, *Annals Phys.* **83** (1974) 491.
- [58] L.P. Csernai and J.I. Kapusta, *Entropy and Cluster Production in Nuclear Collisions*, *Phys. Rept.* **131** (1986) 223.
- [59] T. Herbert, K. Wehrberger and F. Beck, *The Pion propagator in the Walecka model with the delta baryon*, *Nucl. Phys. A* **541** (1992) 699.
- [60] S. Das Gupta, A.Z. Mekjian and M.B. Tsang, *Liquid-gas phase transition in nuclear multifragmentation*, *Adv. Nucl. Phys.* **26** (2001) 89 [[nucl-th/0009033](#)].
- [61] S.R. De Groot, *Relativistic Kinetic Theory. Principles and Applications* (1980).
- [62] L.D. Landau, *The Theory of a Fermi Liquid*, *Zh. Eksp. Teor. Fiz.* **30** (1956) 1058.
- [63] D. Pines, *Theory Of Quantum Liquids: Normal Fermi Liquids*, CRC Press, 1st ed. ed. (1989).
- [64] P. Nozieres, *Theory of interacting Fermi systems*, CRC Press, 1st ed. ed. (1998), [10.1201/9780429495724](#).
- [65] A.J. Leggett, *A theoretical description of the new phases of liquid He-3*, *Rev. Mod. Phys.* **47** (1975) 331.
- [66] G. Baym and S.A. Chin, *Landau Theory of Relativistic Fermi Liquids*, *Nucl. Phys. A* **262** (1976) 527.
- [67] S.P. Klevansky, *The Nambu-Jona-Lasinio model of quantum chromodynamics*, *Rev. Mod. Phys.* **64** (1992) 649.
- [68] A. Schwenk and J. Polonyi, *Towards density functional calculations from nuclear forces*, in *32nd International Workshop on Gross Properties of Nuclei and Nuclear Excitation: Probing Nuclei and Nucleons with Electrons and Photons (Hirschegg 2004)*, 3, 2004 [[nucl-th/0403011](#)].
- [69] E. Epelbaum, H.-W. Hammer and U.-G. Meissner, *Modern Theory of Nuclear Forces*, *Rev. Mod. Phys.* **81** (2009) 1773 [[0811.1338](#)].
- [70] M. Baldo and G.F. Burgio, *Properties of the nuclear medium*, *Rept. Prog. Phys.* **75** (2012) 026301 [[1102.1364](#)].
- [71] B. Friman, K. Hebeler and A. Schwenk, *Renormalization group and Fermi liquid theory for many-nucleon systems*, *Lect. Notes Phys.* **852** (2012) 245 [[1201.2510](#)].
- [72] J.W. Holt, N. Kaiser and W. Weise, *Chiral Fermi liquid approach to neutron matter*, *Phys. Rev. C* **87** (2013) 014338 [[1209.5296](#)].
- [73] J.W. Holt, N. Kaiser and W. Weise, *Nuclear chiral dynamics and thermodynamics*, *Prog. Part. Nucl. Phys.* **73** (2013) 35 [[1304.6350](#)].
- [74] G. Röpke, D.N. Voskresensky, I.A. Kryukov and D. Blaschke, *Fermi liquid, clustering, and structure factor in dilute warm nuclear matter*, *Nucl. Phys. A* **970** (2018) 224 [[1710.08251](#)].
- [75] J.W. Holt, N. Kaiser and T.R. Whitehead, *Tensor Fermi liquid parameters in nuclear matter from chiral effective field theory*, *Phys. Rev. C* **97** (2018) 054325 [[1712.05013](#)].
- [76] B. Friman and W. Weise, *Neutron Star Matter as a Relativistic Fermi Liquid*, *Phys. Rev. C* **100** (2019) 065807 [[1908.09722](#)].

- [77] C. Drischler, J.W. Holt and C. Wellenhofer, *Chiral Effective Field Theory and the High-Density Nuclear Equation of State*, *Ann. Rev. Nucl. Part. Sci.* **71** (2021) 403 [[2101.01709](#)].
- [78] L.V. Delacretaz, Y.-H. Du, U. Mehta and D.T. Son, *Nonlinear bosonization of Fermi surfaces: The method of coadjoint orbits*, *Phys. Rev. Res.* **4** (2022) 033131 [[2203.05004](#)].
- [79] J. Li, T. Guo, J. Zhao and L. He, *Do we need dense matter equation of state in curved spacetime for neutron stars?*, *Phys. Rev. D* **106** (2022) 083021 [[2206.02106](#)].
- [80] A. Sommerfeld, *Zur elektronentheorie der metalle auf grund der fermischen statistik: i. teil: allgemeines, strömungs-und austrittsvorgänge*, *Zeitschrift für Physik* **47** (1928) 1.
- [81] J.I. Kapusta and C. Gale, *Finite-temperature field theory: Principles and applications*, Cambridge Monographs on Mathematical Physics, Cambridge University Press (2011).
- [82] PARTICLE DATA GROUP collaboration, *Review of Particle Physics*, *PTEP* **2022** (2022) [083C01](#).
- [83] T. Chen and T.-Y. Li, *Homotopy continuation method for solving systems of nonlinear and polynomial equations*, *Communications in Information and Systems* **15** (2015) 119.
- [84] K.-l. Wang, S.-x. Qin, Y.-x. Liu, L. Chang, C.D. Roberts and S.M. Schmidt, *Existence and stability of multiple solutions to the gap equation*, *Phys. Rev. D* **86** (2012) 114001 [[1209.2757](#)].
- [85] L.D. Miller and A.E.S. Green, *Relativistic Self-Consistent Meson Field Theory of Spherical Nuclei*, *Phys. Rev. C* **5** (1972) 241.
- [86] K.S. Krane, *Introductory nuclear physics*, John Wiley & Sons (1991).
- [87] G.P. Lepage, *Adaptive multidimensional integration: VEGAS enhanced*, *J. Comput. Phys.* **439** (2021) 110386 [[2009.05112](#)].
- [88] J. Liao and V. Koch, *On the Fluidity and Super-Criticality of the QCD matter at RHIC*, *Phys. Rev. C* **81** (2010) 014902 [[0909.3105](#)].
- [89] L. Du, A. Sorensen and M. Stephanov, *The QCD phase diagram and Beam Energy Scan physics: a theory overview*, *Int. J. Mod. Phys. E* **33** (2024) 2430008 [[2402.10183](#)].
- [90] G. Bertsch, *The collision integral in nuclear matter at zero temperature*, *Zeitschrift für Physik A Atoms and Nuclei* **289** (1978) 103.
- [91] J. Dąbrowski and P. Haensel, *The deformation of the fermi surface in polarized nuclear matter*, *Annals of Physics* **97** (1976) 452.
- [92] T. Frick, H. Muther and A. Sedrakian, *Interaction induced deformation in momentum distribution of spin polarized nuclear matter*, *Phys. Rev. C* **65** (2002) 061303 [[nucl-th/0203048](#)].
- [93] D.B. Kaplan, M.J. Savage and M.B. Wise, *Nucleon - nucleon scattering from effective field theory*, *Nucl. Phys. B* **478** (1996) 629 [[nucl-th/9605002](#)].
- [94] P. Wen, J.W. Holt and M. Li, *Generative Modeling of Nucleon-Nucleon Interactions*, *Phys. Rev. Lett.* **133** (2024) 252501 [[2306.13007](#)].
- [95] W. Ke and Y. Yin, *Does a Quark-Gluon Plasma Feature an Extended Hydrodynamic Regime?*, *Phys. Rev. Lett.* **130** (2023) 212303 [[2208.01046](#)].

- [96] J. Brewer, W. Ke, L. Yan and Y. Yin, *Far-from-equilibrium slow modes and momentum anisotropy in an expanding plasma*, *Phys. Rev. D* **109** (2024) L091504 [[2212.00820](#)].
- [97] W. Ke and Y. Yin, *Non-hydrodynamic response in QCD-like plasma*, *JHEP* **05** (2024) 171 [[2312.08062](#)].
- [98] L. Gavassino, M.M. Disconzi and J. Noronha, *Universality Classes of Relativistic Fluid Dynamics: Foundations*, *Phys. Rev. Lett.* **132** (2024) 222302 [[2302.03478](#)].
- [99] S. Floerchinger, G. Giacalone, L.H. Heyen and L. Tharwat, *Qualifying collective behavior in expanding ultracold gases as a function of particle number*, *Phys. Rev. C* **105** (2022) 044908 [[2111.13591](#)].
- [100] S. Brandstetter et al., *Emergent hydrodynamic behaviour of few strongly interacting fermions*, [2308.09699](#).
- [101] R. Mertig, M. Bohm and A. Denner, *FEYN CALC: Computer algebraic calculation of Feynman amplitudes*, *Comput. Phys. Commun.* **64** (1991) 345.
- [102] V. Shtabovenko, R. Mertig and F. Orellana, *New Developments in FeynCalc 9.0*, *Comput. Phys. Commun.* **207** (2016) 432 [[1601.01167](#)].
- [103] V. Shtabovenko, R. Mertig and F. Orellana, *FeynCalc 9.3: New features and improvements*, *Comput. Phys. Commun.* **256** (2020) 107478 [[2001.04407](#)].